AMERICAN METEOROLOGICAL SOCIETY

Weather, Climate, and Society

EARLY ONLINE RELEASE

This is a preliminary PDF of the author-produced manuscript that has been peer-reviewed and accepted for publication. Since it is being posted so soon after acceptance, it has not yet been copyedited, formatted, or processed by AMS Publications. This preliminary version of the manuscript may be downloaded, distributed, and cited, but please be aware that there will be visual differences and possibly some content differences between this version and the final published version.

The DOI for this manuscript is doi: 10.1175/WCAS-D-11-00007.1

The final published version of this manuscript will replace the preliminary version at the above DOI once it is available.

If you would like to cite this EOR in a separate work, please use the following full citation:

Emanuel, K., 2011: Global Warming Effects on U.S. Hurricane Damage. Wea. Climate Soc. doi:10.1175/WCAS-D-11-00007.1, in press.

© 2011 American Meteorological Society

PRELIMINARY ACCEPTED VERSION

Global Warming Effects on U.S. Hurricane Damage

Kerry Emanuel

Program in Atmospheres, Oceans, and Climate

Room 54-1814, Massachusetts Institute of Technology

77 Massachusetts Avenue

Cambridge, Massachusetts, 02139

(617) 253-2462

emanuel@mit.edu

15 November 2011

Abstract

While many studies of the effects of global warming on hurricanes predict an increase in various metrics of Atlantic basin-wide activity, it is less clear that this signal will emerge from background noise in measures of hurricane damage, which depend largely on rare, high intensity landfalling events and are thus highly volatile compared to basin-wide storm metrics. Using a recently developed hurricane synthesizer driven by large-scale meteorological variables derived from global climate models, we generate 1000 artificial 100-year time series of Atlantic hurricanes that make landfall along the U.S. Gulf and east coasts, for four climate models and for current climate conditions as well as for the warmer climate of 100 years hence under IPCC emissions scenario A1b. These synthetic hurricanes damage a portfolio of insured property, according to an aggregate wind-damage function; damage from flooding is not considered here. Assuming that the hurricane climate changes linearly with time, we create a 1000-member ensemble of time series of property damage. Three of the four climate models used produce increasing damage with time, with the global warming signal emerging on time scales of 40, 113, and 170 years, respectively. We point out, however, that probabilities of damage increase significantly well before such emergence time scales and show that probability density distributions of aggregate damage become appreciably separated from those of the control climate on time scales as short as 25 years. For the fourth climate model, damages decrease with time, but the signal is weak.

1. Introduction

Several lines of evidence suggest that anthropogenic climate change may have a substantial influence on tropical cyclone activity around the world. Global warming generally increases the thermodynamic potential for tropical cyclones (Emanuel, 1987) while changing atmospheric circulation, humidity, and other factors affect both the probability of genesis and the subsequent evolution of the storms (Emanuel, 2007, Vecchi and Soden, 2007). Strictly thermodynamic considerations lead to the expectation that, globally, tropical cyclone frequency should diminish, but the incidence of high intensity events should increase (Emanuel et al., 2008). There is already evidence that the fraction of high intensity storms is indeed increasing (Webster et al., 2005, Elsner et al., 2008), although the global total number of tropical cyclones has not so far exhibited any significant trend (Emanuel, 2005). In the North Atlantic region, where tropical cyclone records are longer and generally of better quality than elsewhere, power dissipation by tropical cyclones is highly correlated with sea surface temperature during hurricane season in the regions where storms typically develop (Emanuel, 2005) and with the difference between the local sea surface temperature and the tropical mean sea surface temperature (Swanson, 2008, Vecchi et al., 2008). The author has argued that in the North Atlantic region, the decadal variations of the sea surface temperature itself appear to be driven mostly by anthropogenic changes in greenhouse gases and aerosols (Mann and Emanuel, 2006, Emanuel, 2008). Other studies hold attribution of past changes in tropical cyclone activity to anthropogenic climate change to be equivocal (Knutson et al., 2010).

Quite a few attempts have been made to use global climate models to make projections of the response of tropical cyclones to global warming. One method simply detects explicitly simulated storms in the models and notes how their levels of activity change with climate. This approach has been taken

by numerous groups (e.g. Bengtsson et al., 1996, Sugi et al., 2002, Oouchi et al., 2006, Yoshimura et al., 2006, Bengtsson et al., 2007) and is becoming more popular as the horizontal resolution of global climate models improves. But even horizontal grid spacing as low as 20 km (Oouchi et al., 2006) cannot resolve the critical eyewall region of the cyclones, and invariably the maximum wind speed of simulated storms is truncated at relatively low values by the lack of horizontal resolution (Zhao et al., 2009). Recent work by Rotunno et al. (2009) suggests that horizontal grid spacing of less than 1 km is needed to properly resolve intense storms. A second approach to the problem is to use statistical relationships between tropical cyclones and large-scale predictors to estimate tropical cyclone activity as a function of variables that are resolved by climate models (e.g. Camargo et al., 2007a, Camargo et al., 2007b). One potential drawback of this approach is that the statistics are trained largely on natural variability, much of which is regional; it is not clear that such indices will perform well when applied to global climate change. Another approach to quantifying the relationship between climate and tropical cyclone activity is to "downscale" tropical cyclone activity from reanalysis or climate model data sets, as pioneered by Knutson et al. (2007) and Emanuel et al. (2008). Such techniques involve running high-resolution, detailed models capable of resolving tropical cyclones, using boundary conditions supplied by reanalysis or climate model data sets. This combines the advantage of relatively robust estimates of large-scale conditions by the reanalyses or climate models with the high fidelity simulation of tropical cyclones by the embedded high-resolution models. As shown by Knutson et al. (2007) and Emanuel et al. (2008), these techniques are remarkably successful in reproducing observed tropical cyclone climatology in the period 1980-2006, particularly in the North Atlantic region, when driven by NCAR-NCEP reanalysis data (Kalnay and co-authors, 1996). A recent comparison between storms produced explicitly in a high-resolution global simulation and those downscaled from the same global model (Emanuel et al., 2010) confirms that even at grid spacing of 14 km, global models truncate the important high-intensity end of

80 the spectrum of tropical cyclones, and reveals substantial differences between the explicit and
81 downscaled storm activity.

82 The general conclusion from all of these studies is that while the global frequency of tropical
83 cyclones is likely to diminish, the frequency of high-intensity events will probably increase as the planet
84 continues to warm (Knutson et al., 2010). Since most wind-related damage is owing to high intensity
85 events, this would imply an increase in wind damage. On the other hand, there is large regional and
86 model-to-model variability in projections of climate change effects on tropical cyclones, so confidence in
87 any regional projections must be correspondingly low. For the North Atlantic, a downscaling of a set of
88 global climate model projections shows that five out of seven of the models predict substantial
89 increases in power dissipation over the 21st century (Emanuel et al., 2008), while a recent downscaling
90 using a comprehensive tropical cyclone model run on a 9-km mesh shows a near doubling of the
91 frequency of high intensity events (Bender et al., 2010). Thus the weight of current evidence suggests a
92 possibly substantial increase in damaging Atlantic hurricanes over the current century, though
93 uncertainty remains large.

94 While basin-wide metrics of tropical cyclone activity show statistically robust changes in the
95 aforementioned model-based projections and may already be evident in observations, there is little
96 evidence for a trend in tropical cyclone-related damage in the U.S (Pielke et al., 2008). This is not
97 surprising, as most wind-related damage is done by tropical cyclones that happen to be at high intensity
98 at the time they make landfall. This is a small subset of all storms over a relatively small fraction of their
99 typical life spans, thus the statistical base of potentially damaging events is small compared to that of
100 the basin-wide set of storms. These findings beg the question of how long it would take for any climate
101 change signal to emerge from background natural variability in damage statistics. This question was
102 addressed recently by Crompton et al. (2011), who concluded that it will take between 120 and 550

years for such a signal to emerge in U.S. tropical cyclone losses. They arrive at their findings using a relationship between normalized losses and Saffir-Simpson category derived from past events, and applying that relationship to projected changes in Atlantic storm activity assuming that fractional changes in the frequency of landfalling events in each category are the same as that of all storms in the North Atlantic. Thus the technique cannot account for possible changes in the tracks of storms, which may change the fraction of all events that make landfall as well as the specific locations of landfall. Moreover, quantization of storms into only five categories, with most of the damage being done by storms of the highest three categories, may alter the signal because it misses changes within categories. (For example, an increase of intensity within category 5, which is open-ended, would presumably cause increased damage even if the number of landfalling category 5 storms remained constant.) These limitations motivate the present study, which applies somewhat different methods to the problem, as described in the next section.

2. Method

Here we apply the tropical cyclone downscaling technique of Emanuel et al. (2008). Briefly, this method embeds a specialized, atmosphere-ocean coupled tropical intensity model in the large-scale atmosphere-ocean environment represented by the global climate model data. The tropical cyclone model is initialized from weak, warm-core vortices seeded randomly in space and time, and whose movement is determined with a beta-and-advection model driven by the flows derived from the climate model daily wind fields. The thermodynamic state used by the intensity model is derived from monthly mean climate model data together with current climatological estimates of ocean mixed layer depths and sub-mixed layer thermal stratification; these ocean parameters are held fixed at their current climatological values. Wind shear, used as input to the intensity model, is likewise derived from the climate model wind fields. In practice, a large proportion of the initial seeds fail to amplify to at least

126 tropical storm strength and are discarded; the survivors are regarded as constituting an estimate of the
127 tropical cyclone climatology for the given climate state.

128 We apply this method to each of four climate models, applying enough seeds to produce 5000
129 U.S. landfalling storms in each case. The models are the CNRM-CM3 model of the Centre National de
130 Recherches Météorologiques, Météo-France; the ECHAM5 model of the Max Planck Institution; the
131 GFDL-CM2.0 model of the NOAA Geophysical Fluids Dynamics Laboratory; and the MIROC 3.2 model of
132 the CCSR/NIES/FRCGC, Japan. We chose these four models from the set of seven models used by
133 Emanuel et al. (2008) which were in turn selected based on the availability of model output needed by
134 the downscaling technique; the four used here are broadly representative of the larger set of seven. We
135 apply the downscaling to simulations of the 20th century climate, using model output for the period
136 1981-2000, and to simulations of a warming climate under IPCC scenario SRES A1b, using model output
137 from the period 2081-2100. We use these synthetic events to construct 1000 stationary time series of
138 100 years length each, representing the climate averaged over 1981-2000 and over 2081-2100,
139 respectively. We construct the time series by randomly drawing, each year, from a Poisson distribution
140 based on the overall annual frequency of events in the set. The 1000-member ensemble is created by
141 repeating the process using different random draws from the Poisson distribution each year. Thus we
142 have 1000 100-year time stationary series for each of four climate models for each of two time frames.
143 As detailed below, we will use these time series to create 1000 100-year time series of damage in an
144 evolving climate by linearly combining the two stationary time series sets with a weighting that varies
145 linearly in time.

146 We note here that the intent is to distinguish climate change-induced trends from background
147 short-term random variability. We do not attempt to account for other sources of systematic climate
148 change, such as changing solar or volcanic activity, or long-period natural variability, such as the Atlantic
149 Multidecadal Oscillation (AMO); in this respect we use the same assumptions as did Crompton et al.

150 (2011). We simply note that detecting any signal of anthropogenic climate change, not just one that
151 might be present in tropical cyclone statistics, requires one to account for other forced changes, and
152 that long-period natural variability, such as the AMO, cannot meaningfully be considered noise in this
153 context. If it exists and is important, its influence can, in principle, be quantified and accounted for; if it
154 cannot be quantified then one must give up on any exercise in climate change attribution on these time
155 scales.
156
157 Next, we allow the simulated storms to interact with a portfolio of insured property: the
158 Industry Exposure Database, produced by Risk Management Solutions Inc[1]. This consists of estimates of
159 total insured values for each zip code and county in the U.S. and for each postcode in Europe, using
160 sampled company premium information, census demographics and economics data, building square
161 footage data, and representative policy terms and conditions. These total insured values and other
162 variables are then aggregated into 100 zones distributed along the U.S. Gulf and east coasts, whose
163 locations are shown in Figure 1[2]. These locations represent roughly the population-weighted
164 geographical centers of the zones. For simplicity, we model the damage in a given zone according to the
165 wind experienced at the position of the zone center. For each tropical cyclone event, we use a wind
166 damage function, described presently, to estimate the fractional loss of value at in each zone, and
167 multiply this by the total insured value of property in that zone. This gives an estimate of the total
168 amount of damage in U.S dollars caused by each event in each zone; the total insured damage from an
169 event is then the sum of this quantity over all zones. A drawback of this approach is that aggregating the
170 building values into zones represented by points will make the damage more volatile than it should be,
171 as some strong storms will pass between the zone centers and do little damage there, whereas in reality

[1] http://www.rms.com/Catastrophe/Models/us_industry_exposure.asp
[2] The original data is proprietary, and this aggregation was done by the provider to allow it to be used for the present purpose.

some of the insured property between zone centers will experience high winds. This increased volatility will decrease the climate signal-to-noise ratio and make the damage probability density functions broader than they ought to be.

Property damage from wind storms is observed to increase quite rapidly with wind speed. Empirical studies relating wind to damage suggest a high power-law dependence of damage on wind speed (Pielke, 2007) . For example, Nordhaus (2010) estimates that damage varies as the ninth power of wind speed for wind damage in the U.S. In reality, most structures in the U.S. and many other countries are built to withstand frequently encountered winds; it is highly unlikely, for example, that a wind of 20 knots would do any damage at all. Thus we consider a damage function that produces positive values only for winds speeds in excess of a specified threshold. On physical grounds, we expect that damage should vary as the cube of the wind speed over a threshold value. Finally, we require that the fraction of the property damaged approach unity at very high wind speeds; in any event, we cannot allow it to exceed unity. A plausible function that meets these requirements is

$$f = \frac{v_n^3}{1+v_n^3}, \tag{1}$$

where f is the fraction of the property value lost and

$$v_n \equiv \frac{\mathrm{MAX}\left[\left(V - V_{thresh}\right), 0\right]}{V_{half} - V_{thresh}},$$

with V the wind speed, V_{thresh} is the wind speed at and below which no damage occurs, and V_{half} is the wind speed at which half the property value is lost. This function is plotted in Figure 2, for $V_{thresh} = 50\ kts$ and two values of V_{half} . These functions are highly idealized; in reality, property damage depends on much more than the peak wind speed experienced during a storm; for example, the

direction of the wind, its degree of gustiness, and the duration of damaging winds all influence the amount of damage. Also, we do not consider damage from freshwater flooding or storm surge, though the latter is, to some extent, also a nonlinear function of wind speed. The damage functions illustrated in Figure 2 can be compared to damage functions derived from theory and from insurance claims data as reviewed by Watson and Johnson (2004). By varying V_{half}, we will explore the sensitivity of the results to the damage function.

Using this damage function and the property values from the Industry Exposure Database in conjunction with the two synthetic tropical cyclone events sets for each of the four models, we derive 1000 100-year time series of U.S insured property damage for each model and for each of the two climates considered. Then, for each ensemble member, we blend the two 100-year time series representing the two climates into a single time series by linearly combining the two damage amounts assuming that the transition from one climate to the other occurs linearly over 100 years; thus the damage in each year is a weighted average of the damage from each climate state, with the weight varying linearly with time. This results in 1000 100-year time series for each of the 4 models, each representing a transitioning climate. We use these time series to evaluate the emergence of global warming signals. As in the work of Crompton et al. (2011), we assume that the noise against which the global warming signal is measured is random variability on time scales ranging up to a few years (including, for example, ENSO-related variability) but not natural multidecadal variability. We also consider that changes in damage owing to changing distributions of property and property value are quantifiable after-the-fact and thus do not constitute noise in the system.

3. Results

Figure 3 shows property damage each year for a single ensemble member of the GFDL 20th century climate simulation, using the damage function (1) with $V_{half} = 150\ kts$. As expected, damage is highly

volatile, ranging from a few million to 275 million dollars. Figure 4 again shows a single randomly chosen ensemble member of property damage but for the blended time series in which the climate state transitions linearly from its late 20th century condition to its late 21st century condition under IPCC emissions scenario A1b. In this particular case, an upward trend in damage seems evident, though the trend is not large compared to the interannual variance. Figure 5 presents a different metric: damage accumulated over every year from 2000 to the year on the x axis, for a single ensemble member in each of the constant 20th century climate and the transitioning climate. (The standard deviations up and down from the ensemble means are also shown for comparison.) Accumulating the damage has the effect of smoothing over interannual variations and the difference in the trends becomes clear after a few decades.

The probability densities of damage, derived using the 1000-member ensemble of accumulated damage at various times, are shown for all four models in Figure 6. In most cases, the probability densities of the warming climate are distinct from those of the current climate by 100 years out. Note that in the case of the MIROC model, the probability densities shift toward lower damage amounts as the climate warms.

We also calculate the time scale over which the global warming signal may be considered to have emerged in time series of damage. Following Bender et al. (2010) and Crompton et al. (2011), we define the emergence time scale as that time after which fewer than 5% of the linear regression slopes of damage up to that time, amongst the 1000-member ensemble, are negative. In the case of the GFDL CM2.0-derived damage time series, this occurs at 40 years. In the other cases, it does not occur within the 100-year time frame of the time series. In these cases, we artificially extend the time series of each of the 1000-members of the ensemble by extrapolating the linear damage trend forward another 100 years. Figure 7 shows an example of the fraction of regression slopes that are negative, as a function of

the length of time over which the regression is carried out. It can be shown that if the interannual variance of property damage (the "noise") is Gaussian, and the underlying trend is linear, then the fraction of negative slopes as a function of the length of the series should be a cumulative distribution function (cdf) formed from a normal distribution; for this reason we also show a fit of such a cdf to the data. With the time series extrapolated out to 200 years, the global warming signal in property damage emerges from background noise in 113 years for the CNRM model and 170 years for the ECHAM 5 model. The negative signal present in the MIROC model does not emerge within the 200-year time frame.

How sensitive are these results to the damage function used? As a first step in addressing this issue, we repeated the analysis using $V_{half} = 110\ kts$ in (1), as illustrated by the dashed curve in Figure 2. Figure 8 shows the result for the CNRM simulation; this should be compared to Figure 6c. Aside from the obvious increase in the magnitude of the damage, the shape of the probability distributions and their separation with climate change is hardly distinguishable. The emergence time scale remains identical at 113 years. This lack of sensitivity to details of the damage function pertains to the other models as well.

4. Discussion

For the three global climate models that produce increasing damage in the U.S., the time scales for trends in damage to emerge from background noise range from 40 to 170 years, somewhat shorter than those reported in Crompton et al. (2011). There are several potential reasons for this, including our use of a different suite of global models and that fact that Crompton et al. (2011) assumed a proportionality between basin-wide and landfalling activity and estimated changes in damages by changes in the distribution of events within the limited 5-bin Saffir-Simpson categorization.

We caution that the question of when a statistically robust trend can be detected in damage time series should not be confused with the question of when climate-induced changes in damage become a significant consideration. Policies and other actions that address U.S. hurricane damage on the time scale of decades would surely distinguish the probabilistic outcome represented by, say, the 25 year probability density of a warming climate given in Figure 6a from that of the steady climate at the same lead time. Thus if climate change effects are anticipated, or detected in basin-wide storm statistics, sensible policy decisions should depend on the projected overall shift in the probability of damage rather than on a high-threshold criterion for trend emergence. This is particularly important in view of evidence that suggests that an anthropogenic climate change signal has already emerged in Atlantic hurricane records (Mann and Emanuel, 2006).

A number of caveats apply to the present analysis. First, we have held constant the distribution and value of insured property, not accounting for changing demographics or adaptation strategies that might reduce vulnerability to damage. We do not consider the effects of rising sea-level, which would increase vulnerability to damage by storm surges. Nor have we taken into account any changing incidence of freshwater flooding stemming from tropical cyclone rainfall. We have relied for this study on a single projected emissions scenario, SRES A1b, and the results obviously depend rather sensitively on the global climate model used to drive the downscaling. At the same time, the downscaling method itself is, no doubt, an imperfect measure of the tropical cyclone climatology that would attend a particular climate state.

5. Summary

We used a synthetic tropical cyclone generator to produce 1000 artificial time series of U.S. landfalling Atlantic hurricanes, each of 100 years length for the climate of the late 20th century and for the late 21st century, using four climate models. Some of the tropical cyclones affect properties

282 contained in a portfolio of insured property, and a damage function was used to predict how much
283 damage each storm would do to these properties. This results in two 1000-member ensembles of 100-
284 year times series of property damage for each of the four models: one for the climate of the late 20th
285 century and one for the climate of the late 21st century under IPCC emissions scenario SRES A1b. These
286 two were blended together, assuming a linear variation of climate over the 21st century, to create time
287 series of property damage representing a transitioning climate. From these times series one can make
288 inferences concerning the effect of anthropogenic climate change on U.S. hurricane wind-related
289 property damage that also account for the high level of background noise inherent in the volatile
290 statistics of intense landfalling tropical cyclones.

291 For three of the four climate models downscaled, damages increase as a result of projected global
292 warming, but the fourth model shows a small decrease of damage with time. For the three climate
293 models that have increasing damage, the climate change signal emerges from background variability,
294 according to a recently published criterion, on time scales of 40, 113, and 170 years, respectively; the
295 decreasing signal of the fourth model is not clearly distinguishable from noise even after 200 years. On
296 the other hand, the probability distributions of damage in a warming climate become distinguished
297 from those of background climate in as little as 25 years, thus we argue that those concerned with
298 future U.S. country-wide tropical cyclone damage on decadal time scales would be well advised to
299 include climate change as a consideration.

300

301 *Acknowledgements:* The author thanks Risk Management Solution, Inc. for making available their
302 proprietary Industry Exposure Database, and Alan Lange for processing this data. This research was
303 supported by the National Oceanographic and Atmospheric Administration under grant
304 NA090AR4310131.

References

Bender, M. A., T. R. Knutson, R. E. Tuleya, J. J. Sirutis, G. A. Vecchi, S. T. Garner, and I. M. Held, 2010: Modeled impact of anthropogenic warming on the frequency of intense Atlantic hurricanes. *Science,* **327,** 454-458

Bengtsson, L., M. Botzet, and M. Esch, 1996: Will greenhouse-induced warming over the next 50 years lead to higher frequency and greater intensity of hurricanes? *Tellus,* **48A,** 57-73.

Bengtsson, L., K. I. Hodges, M. Esch, N. Keenlyside, L. Kornbleuh, J.-J. Luo, and T. Yamagata, 2007: How may tropical cyclones change in a warmer climate? *Tellus,* **59,** 539-561.

Camargo, S. J., K. A. Emanuel , and A. H. Sobel, 2007a: Use of a genesis potential index to diagnose ENSO effects on tropical cyclone genesis. *J. Climate,* **20,** 4819-4834.

Camargo, S. J., A. H. Sobel, A. G. Barnston, and K. A. Emanuel 2007b: Tropical cyclone genesis potential index in climate models. *Tellus A,* **59,** 428-443.

Crompton, R. P., R. A. Pielke, Jr., and J. K. McAneney, 2011: Emergence time scales for detection of anthropogenic climate change in US tropical cyclone loss data. *Environ. Res. Let.,* in press.

Elsner, J. B., J. P. Kossin, and T. H. Jagger, 2008: The increasing intensity of the strongest tropical cyclones. *Nature* **455,** 92-95.

Emanuel, K., 1987: The dependence of hurricane intensity on climate. *Nature,* **326,** 483-485.

____, 2005: Increasing destructiveness of tropical cyclones over the past 30 years. *Nature,* **436,** 686-688.

____, 2007: Environmental factors affecting tropical cyclone power dissipation. *J. Climate,* **20,** 5497-5509.

____, 2008: The hurricane-climate connection. *Bull. Amer. Meteor. Soc.,* **89,** ES10-ES20.

Emanuel, K., R. Sundararajan, and J. Williams, 2008: Hurricanes and global warming: Results from downscaling IPCC AR4 simulations. *Bull. Amer. Meteor. Soc.,* **89,** 347-367.

Emanuel, K., K. Oouchi, M. Satoh, H. Tomita, and Y. Yamada, 2010: Comparison of explicitly simulated and downscaled tropical cyclone activity in a high-resolution global climate model. *J. Adv. Model. Earth Sys.,* **2,** DOI:10.3894/JAMES.2010.2.9

Kalnay, E., and co-authors, 1996: The NCEP/NCAR 40-year reanalysis project. *Bull. Amer. Meteor. Soc.,* **77,** 437-471.

Knutson, T. R., J. J. Sirutis, S. T. Garner, I. M. Held, and R. E. Tuleya, 2007: Simulation of the recent multi-decadal increase of Atlantic hurricane activity using an 18-km grid regional model. *Bull. Amer. Meteor. Soc.,* **88,** 1549-1565.

Knutson, T. R.et al., 2010: Tropical cyclones and climate change. *Nature Geosci.,* **3,** 157-163.

Mann, M. E., and K. A. Emanuel, 2006: Atlantic hurricane trends linked to climate change. *EOS,* **87,** 233-244.

Nordhaus, W. D., 2010: The economics of hurricanes and implications of global warming. *Clim. Change Econ.,* **1,** 1-20.

Oouchi, K., J. Yoshimura, H. Yoshimura, R. Mizuta, S. Kusonoki, and A. Noda, 2006: Tropical cyclone climatology in a global-warming climate as simukated in a 20 km-mesh global atmospheric model: Frequency and wind intensity analyses. *J. Meteor. Soc. Japan,* **84,** 259-276.

Pielke, R. A., Jr., 2007: Future economic damage from tropical cyclones: sensitivities to societal and climate changes. *Phil. Trans. Roy. Soc.,* **365,** 1-13.

Pielke, R. A., Jr., J. Gratz, C. W. Landsea, D. Collins, M. A. Saunders, and R. Musulin, 2008: Normalized hurricane damage in the United States: 1900-2005. *Nat. Hazards Rev.,* **9,** 29-42.

Rotunno, R., Y. Chen, W. Wang, C. Davis, J. Dudhia, and C. L. Holland, 2009: Large-eddy simulation of an idealized tropical cyclone. *Bull. Amer. Meteor. Soc.,* **90,** 1783-1788.

352 Sugi, M., A. Noda, and N. Sato, 2002: Influence of the global warming on tropical cyclone climatology: An
353 experiment with the JMA global climate model. *J. Meteor. Soc. Japan,* **80,** 249-272.
354 Swanson, K., 2008: Nonlocality of Atlantic tropical cyclone intensities. *Geochem. Geophys. Geosys.,* **9,**
355 doi:10.1029/2007GC001844
356 Vecchi, G. A., and B. J. Soden, 2007: Increased tropical Atlantic wind shear in model projections of global
357 warming. *Geophys. Res. Lett. ,* **34,** L08702, doi:08710.01029/02006GL028905.
358 Vecchi, G. A., K. Swanson, and B. J. Soden, 2008: Whither hurricane activity? . *Science,* **322,** 687-689.
359 Watson, C. C., and M. E. Johnson, 2004: Hurricane loss estimation models: Opportunities for improving
360 the state of the art. *Bull. Amer. Meteor. Soc.,* **85,** DOI:10.1175/BAMS-85
361 Webster, P. J., G. J. Holland, J. A. Curry, and H.-R. Chang, 2005: Changes in tropical cyclone number,
362 duration and intensity in a warming environment. *Science,* **309,** 1844-1846.
363 Yoshimura, J., S. Masato, and A. Noda, 2006: Influence of greenhouse warming on tropical cyclone
364 frequency. *J. Meteor. Soc. Japan,* **84,** 405-428.
365 Zhao, M., I. M. Held, S.-J. Lin, and G. A. Vecchi, 2009: Simulations of global hurricane climatology,
366 interannual variability, and response to global warming using a 50km resolution GCM. *J. Climate,*
367 **22,** 6653–6678.

368
369
370

371

372 **Figure Captions**

373 **Figure 1:** Locations of zone centers (blue dots) used for estimating hurricane damage.

374 **Figure 2:** Fraction of property value lost as a function of winds speed using equation (1) with

375 $V_{thresh} = 50\ kts$ and $V_{half} = 150\ kts$ (solid) and $V_{half} = 110\ kts$ (dashed).

376 **Figure 3:** Property damage ($ millions U.S.) each year for a single ensemble member of the GFDL CM2.0

377 model with climate held fixed at its 1981-2000 mean condition.

378 **Figure 4:** Same a Figure 3 but for a climate transitioning linearly from its state at the end of the 20th

379 century to its state at the end of the 21st century.

380 Figure 5: Accumulated damage from 2000 to the year on the abscissa, from the same two ensemble

381 members presented respectively in Figures 3 and 4. The error bars shows one standard deviation up

382 and down from the ensemble mean.

383 **Figure 6:** Probability density of accumulated property damage, across the 1000-member ensemble at

384 various times as indicated, for the GFDL CM2.0 model (a), The ECHAM5 model (b), the CNRM model (c)

385 and the MIROC model (d). Blue curves indicate constant 20th century climate, while the red curves

386 shows results for the warming climate.

387 **Figure 7:** Percentage of ensembles members with negative linear regression slopes, as a function of the

388 ending time of the time series, for the CNRM damage projections (blue). The red curve represents a fit

389 to the data of a cumulative distribution function based on a normal distribution. The emergence time

390 scale is defined as the time after which negative slopes constitute less than 5% of the total; in this case,

391 this occurs in year 2113.

392 **Figure 8:** Same as Figure 6c but using the damage function given by (1) using $V_{half} = 110\ kts$.

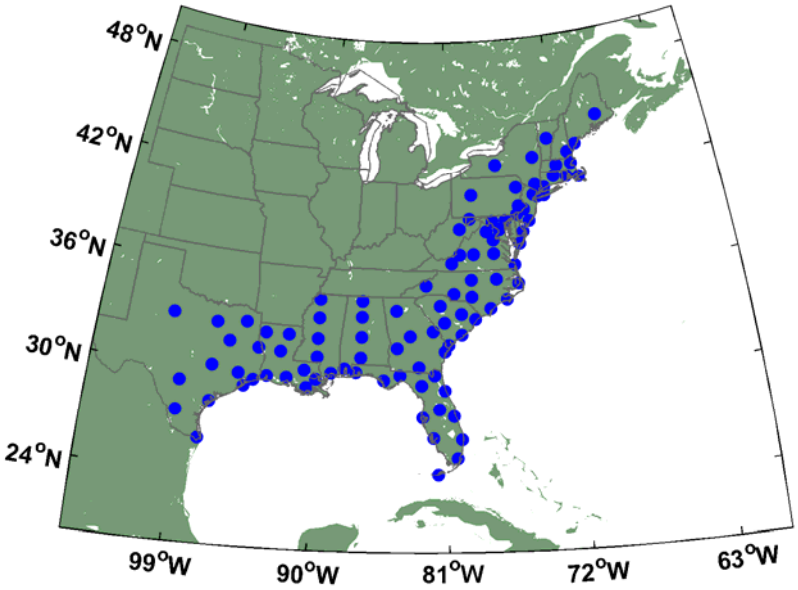

Figure 1: Locations of zone centers (blue dots) used for estimating hurricane damage.

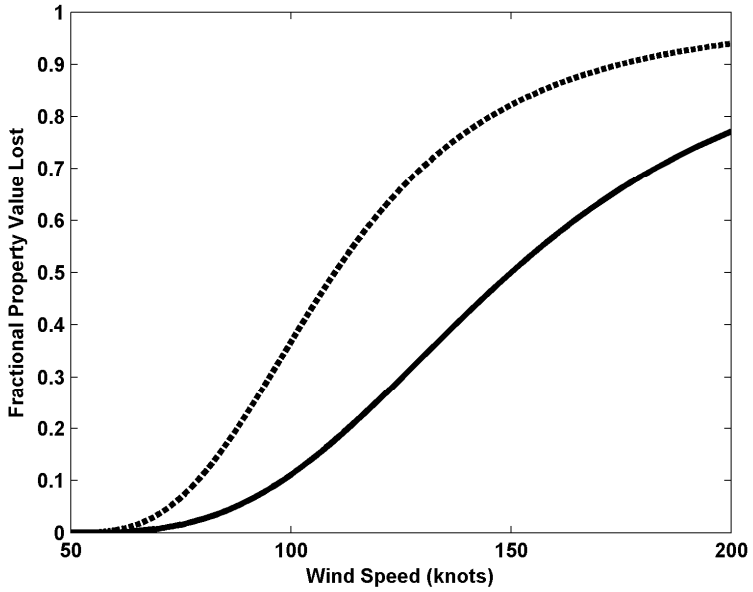

Figure 2: Fraction of property value lost as a function of winds speed using equation (1) with $V_{thresh} = 50\ kts$ and $V_{half} = 150\ kts$ (solid) and $V_{half} = 110\ kts$ (dashed).

403

404

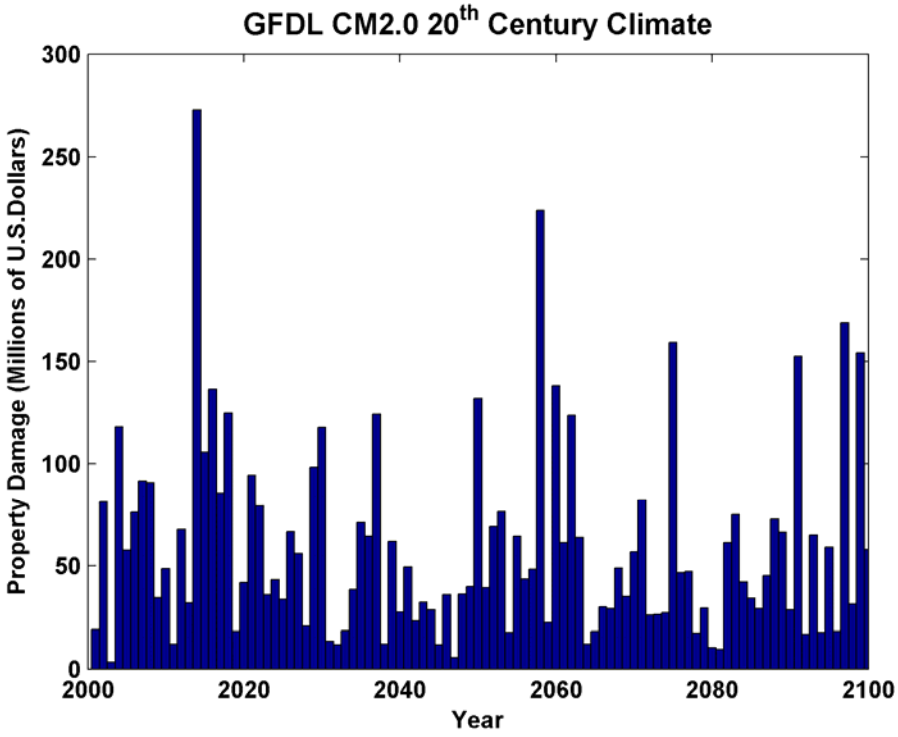

405

406 **Figure 3: Property damage ($ millions U.S.) each year for a single ensemble member of the GFDL CM2.0 model with climate**
407 **held fixed at its 1981-2000 mean condition.**

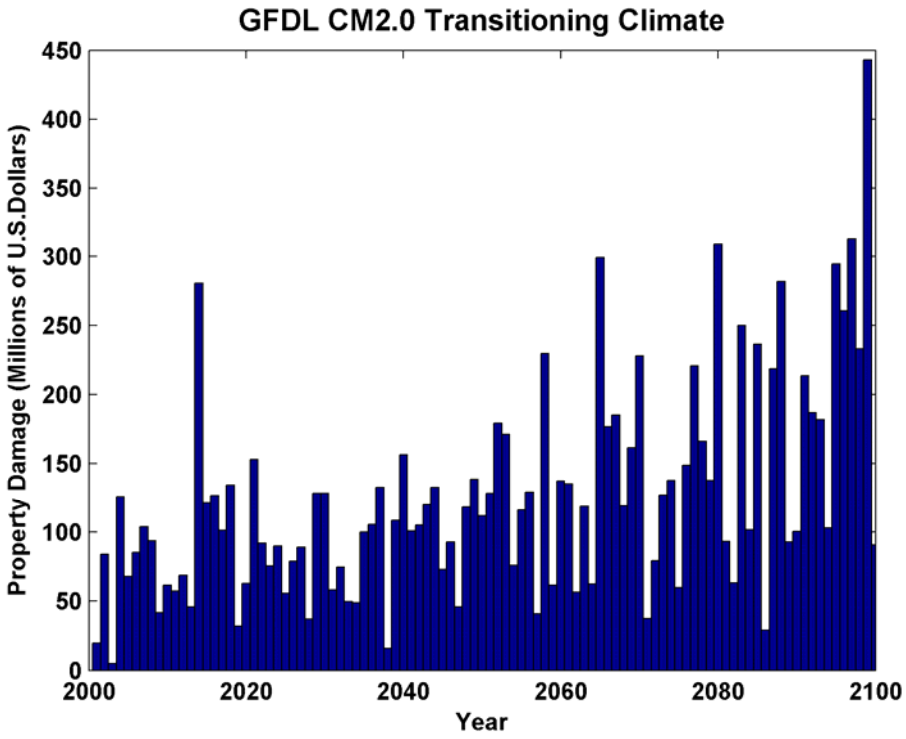

Figure 4: Same a Figure 3 but for a climate transitioning linearly from its state at the end of the 20th century to its state at the end of the 21st century.

412

413

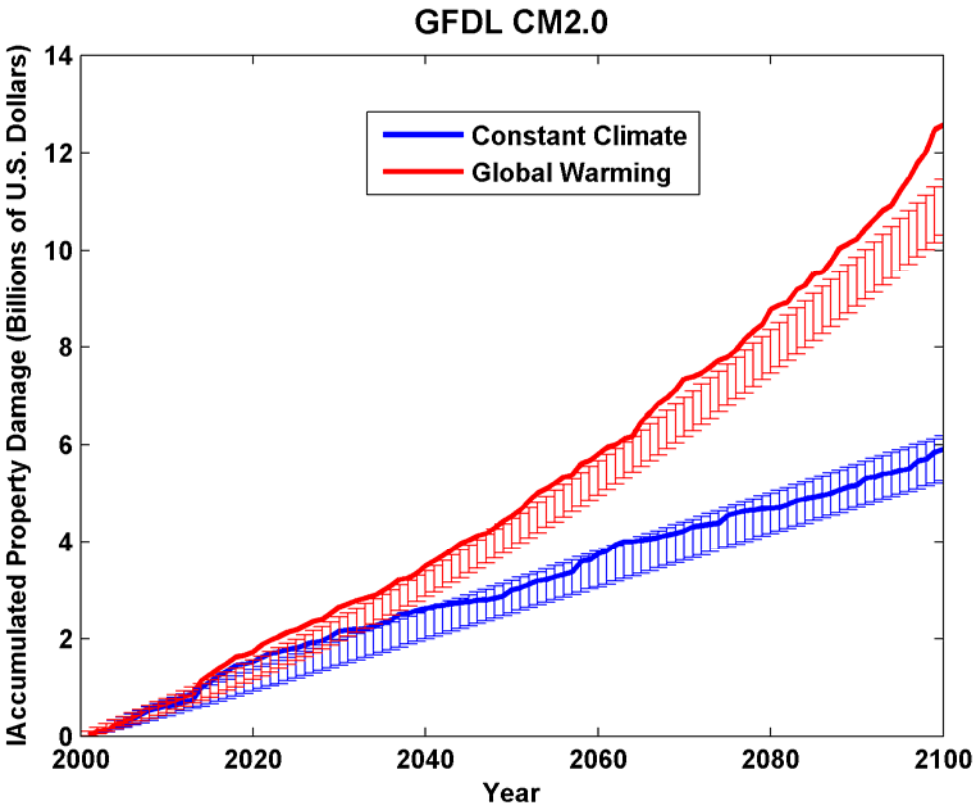

414

415 **Figure 5: Accumulated damage from 2000 to the year on the abscissa, from the same two ensemble members presented**
416 **respectively in Figures 3 and 4. The error bars shows one standard deviation up and down from the ensemble mean.**

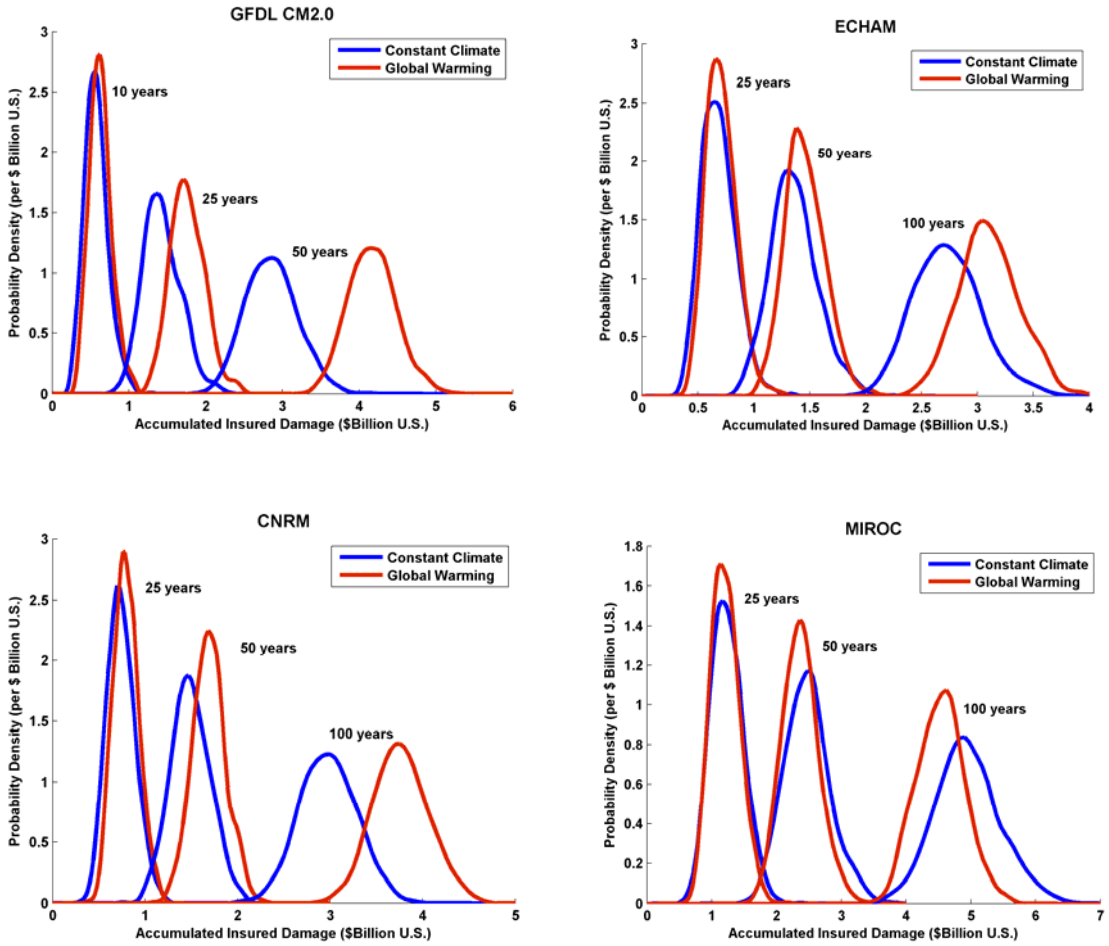

Figure 6: Probability density of accumulated property damage, across the 1000-member ensemble at various times as indicated, for the GFDL CM2.0 model (a), The ECHAM5 model (b), the CNRM model (c) and the MIROC model (d). Blue curves indicate constant 20th century climate, while the red curves shows results for the warming climate.

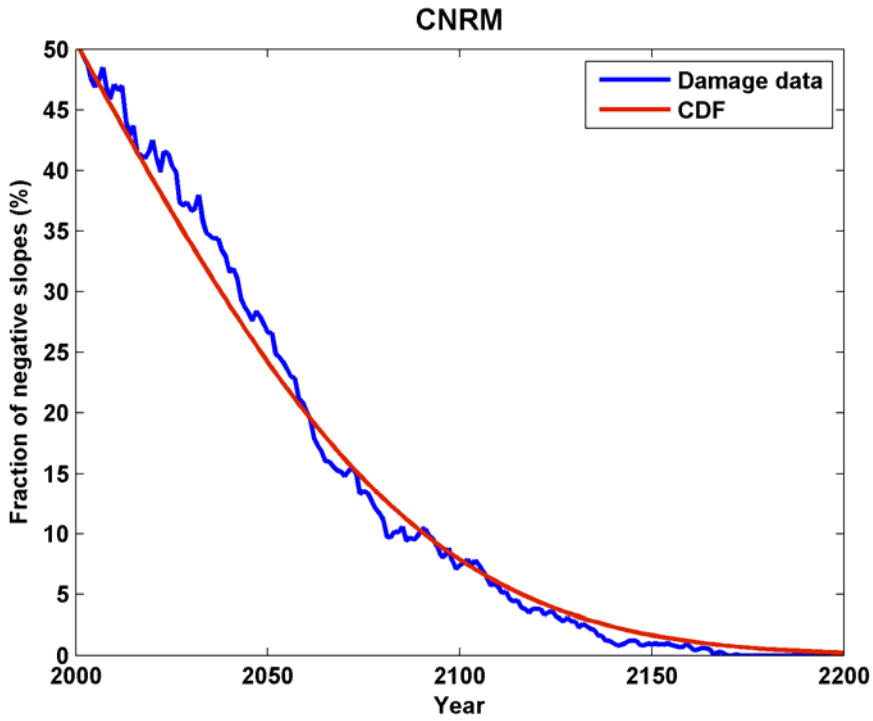

Figure 7: Percentage of ensembles members with negative linear regression slopes, as a function of the ending time of the time series, for the CNRM damage projections (blue). The red curve represents a fit to the data of a cumulative distribution function based on a normal distribution. The emergence time scale is defined as the time after which negative slopes constitute less than 5% of the total; in this case, this occurs in year 2113.

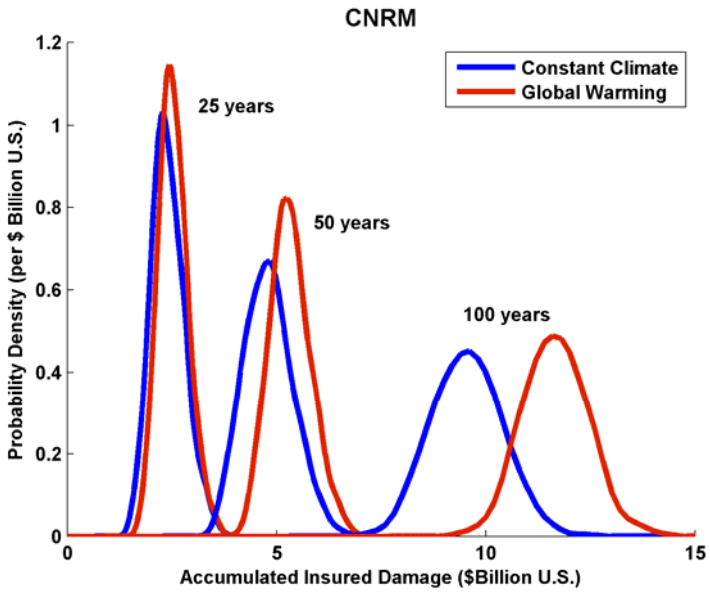

Figure 8: Same as Figure 6c but using the damage function given by (1) using $V_{half} = 110\ kts$.